One-dimensional frequency-based spectroscopy

Agata Cygan,[1,*] **Piotr Wcisło,**[1] **Szymon Wójtewicz,**[1] **Piotr Masłowski,**[1] **Joseph T. Hodges,**[2] **Roman Ciuryło,**[1] **and Daniel Lisak**[1]

[1]*Institute of Physics, Faculty of Physics, Astronomy and Informatics, Nicolaus Copernicus University in Torun, Grudziadzka 5, 87-100 Torun, Poland.*

[2] *National Institute of Standards and Technology, 100 Bureau Drive, Gaithersburg, Maryland 20899, USA*

**agata@fizyka.umk.pl*

Abstract: Recent developments in optical metrology have tremendously improved the precision and accuracy of the horizontal (frequency) axis in measured spectra. However, the vertical (typically absorbance) axis is usually based on intensity measurements that are subject to instrumental errors which limit the spectrum accuracy. Here we report a one-dimensional spectroscopy that uses only the measured frequencies of high-finesse cavity modes to provide complete information about the dispersive properties of the spectrum. Because this technique depends solely on the measurement of frequencies or their differences, it is insensitive to systematic errors in the detection of light intensity and has the potential to become the most accurate of all absorptive and dispersive spectroscopic methods. The experimental results are compared to measurements by two other high-precision cavity-enhanced spectroscopy methods. We expect that the proposed technique will have significant impact in fields such as fundamental physics, gas metrology and environmental remote sensing.

OCIS codes: (120.6200) Spectrometers and spectroscopic instrumentation; (140.3425) Laser stabilization; (140.3570) Lasers, single-mode; (260.2030) Dispersion; (300.1030) Absorption; (300.3700) Linewidth; (300.6320) Spectroscopy, high-resolution.

References and links

1. T. Udem, A. Huber, B. Gross, J. Reichert, M. Prevedelli, M. Weitz, and T. W. Hänsch,“ Phase-coherent measurement of the hydrogen 1S-2S transition frequency with an optical frequency interval divider chain,” Phys. Rev. Lett. **79**, 2646 (1997).
2. E. J. Salumbides, J. C. J. Koelemeij, J. Komasa, K. Pachucki, K. S. E. Eikema, and W .Ubachs “Bounds on fifth forces from precision measurements of molecules,” Phys. Rev. D **87**, 112008 (2013).
3. C. E. Miller, L. R. Brown, R. A. Toth, D. Chris Benner, and V. Malathy Devi, “Spectroscopic challenges for high accuracy retrievals of atmospheric CO_2 and the Orbiting Carbon Observatory (OCO) experiment,” C. R. Phys. **6**, 876-887 (2005).
4. R. Monastersky, “Global carbon dioxide levels near worrisome milestone,” Nature **497**, 13-14 (2013).
5. L. Moretti, A. Castrillo, E. Fasci, M. D. De Vizia, G. Casa, G. Galzerano, A. Merlone, P. Laporta, and L. Gianfrani, “Determination of the Boltzmann constant by means of precision measurements of $H_2^{18}O$ line shapes at 1.39 um,” Phys. Rev. Lett. **111**, 060803 (2013).
6. W. Ubachs, R. Buning, K. S. E. Eikema, and E. Reinhold, “On a possible variation of the proton-to-electron mass ratio: H_2 spectra in the line of sight of high-redshift quasars and in the laboratory,” J. Mol. Spectrosc. **241**, 155-179 (2007).
7. K. G. Libbrecht, and M. W. Libbrecht, “Interferometric measurement of the resonant absorption and refractive index in rubidium gas,” Am. J. Phys. **74**, 1055-1060 (2006).

#237196 - $15.00 USD Received 31 Mar 2015; revised 6 May 2015; accepted 11 May 2015; published 22 May 2015

8. K. Nakagawa, T. Katsuda, A. S. Shelkovnikov, M. de Labachelerie, and M. Ohtsu, "Highly sensitive detection of molecular absorption using a high finesse optical cavity," Opt. Commun. **107**, 369-327 (1994).
9. R. W. P. Drever, J. L. Hall, F. V. Kowalski, J. Hough, G. M. Ford, A. J. Munley, and H. Ward, "Laser phase and frequency stabilization using an optical resonator," Appl. Phys. B **31**, 97-105 (1983).
10. D. Lisak, A. Cygan, K. Bielska, M. Piwiński, F. Ozimek, T. Ido, R. S. Trawiński, and R. Ciuryło, "Ultra narrow laser for optical frequency reference," Acta Phys. Pol. A **121**, 614-621 (2012).
11. A. Cygan, D. Lisak, P. Morzyński, M. Bober, M. Zawada, E. Pazderski, and R. Ciuryło, "Cavity mode-width spectroscopy with widely tunable ultra narrow laser," Opt. Express **21**, 29744-29754 (2013).
12. G.-W. Truong, K. O. Douglass, S. E. Maxwell, R. D. van Zee, D. F. Plusquellic, J. T. Hodges, and D. A. Long, "Frequency-agile, rapid scanning spectroscopy," Nat. Photon. **7**, 532-534 (2013).
13. D. A. Long, G.-W. Truong, R. D. van Zee, D. F. Plusquellic, and J. T. Hodges, "Frequency-agile, rapid scanning spectroscopy: absorption sensitivity of 2×10^{-12} $\mathrm{cm}^{-1}\mathrm{Hz}^{-1/2}$ with a tunable diode laser," Appl. Phys. B **114**, 489-495 (2014).
14. W. R. Bennett, "Hole burning effects in a He-Ne optical maser," Phys. Rev. **126**, 580-593 (1962).
15. R. A. McFarlane, "Frequency pushing and frequency pulling in a He-Ne gas optical maser," Phys. Rev. Lett. **135**, A543-A550 (1964).
16. D. D. Smith, K. Myneni, J. A. Odutola, and J. C. Diels, "Enhanced sensitivity of a passive optical cavity by an intracavity dispersion medium," Phys. Rev. A **80**, 011809(R) (2009).
17. G. C. Bjorklund, "Frequency modulation spectroscopy: a new method for measuring weak absorptions and dispersions," Opt. Lett. **5**, 15-17 (1980).
18. G. C. Bjorklund, M. D. Levenson, W. Lenth, and C. Oritz, "Frequency modulation (FM) spectroscopy: theory of lineshapes and signal-to-noise analysis," Appl. Phys. B **32**, 145-152 (1983).
19. J. Ye, L.-S. Ma, and J. L. Hall, "Ultrasensitive detections in atomic and molecular physics: demonstration in molecular overtone spectroscopy," J. Opt. Soc. Am. B **15**, 6-15 (1998).
20. S. A. Diddams, J.-C. Diels, and B. Atherton, "Differential intracavity phase spectroscopy and its application to a three-level system in samarium," Phys. Rev. A **58**, 2252 (1998).
21. J.-M. Hartmann, C. Boulet, and D. Robert, *Collisional Effects on Molecular Spectra: Laboratory Experiments and Model, Consequences for Applications* (Elsevier, Amsterdam 2008).
22. Ch. Salomon, D. Hils, and J. L. Hall, "Laser stabilization at the milihertz level," J. Opt. Soc. Am. B **5**, 1576-1587 (1988).
23. T. Kessler, C. Hagemann, C. Grebing, T. Legero, U. Sterr, F. Riehle, M. J. Martin, L. Chen, and J. Ye, "A sub-40-mHz-linewidth laser based on a silicon single-crystal optical cavity," Nat. Photon. **6**, 687-692 (2012).
24. A. Cygan, P. Wcisło, S. Wójtewicz, P. Masłowski, R. S. Trawiński, R. Ciuryło, and D. Lisak, "Alternative approaches to cavity enhanced absorption spectroscopy," J. Phys.: Conf. Ser. **548**, 012024 (2014).
25. J. T. Hodges, D. A. Long, A. Fleisher, K. Bielska, and S. Wójtewicz, "Mode-resolved absorption and dispersion measurements in high-finesse cavities," in *Imaging and Applied Optics 2014*, OSA Technical Digest (Optical Society of America, 2014), paper LW3D.3.
26. J. Y. Wang, P. Ehlers, I. Silander, and O. Axner, "Speed-dependent effects in dispersion mode of detection and in noise-immune cavity-enhanced optical heterodyne molecular spectrometry: experimental demonstration and validation of predicted line shape," J. Opt. Soc. Am. B **29**, 2980-2989 (2012).
27. J. Y. Wang, P. Ehlers, I. Silander, J. Westberg, and O Axner, "On the accuracy of the assessment of molecular concentration and spectroscopic parameters by frequency modulation spectrometry and NICE-OHMS," J. Quant. Spectrosc. Radiat. Transfer **136**, 28-44 (2014).
28. K. K. Lehmann, "Dispersion and Cavity Ring Down spectroscopy," in *Cavity-Ringdown Spectroscopy-An Ultratrace-Absorption Measurement Technique* (ACS Books, 1999), pp. 106-124.
29. R. Ciuryło, "Shapes of pressure- and Doppler-broadened spectral lines in the core and near wings," Phys. Rev. A **58**, 1029 (1998).
30. K.-E. Peiponen and J. J. Saarinen, "Generalized Kramers-Kronig relations in nonlinear optical- and THz-spectroscopy," Rep. Prog. Phys. **72**, 056401 (2009).
31. T. W. Hänsch, "Nobel Lecture: Passion for precision," Rev. Mod. Phys. **78**, 1297-1309 (2006).
32. J. T. Hodges, H. P. Layer, W. M. Miller, and G. E. Scace, "Frequency-stabilized single-mode cavity ring-down apparatus for high-resolution absorption spectroscopy," Rev. Sci. Instrum. **75**, 849-863 (2004).
33. J. Morville, S. Kassi, M. Chenevier, and D. Romanini, "Fast, low-noise, mode-by-mode, cavity-enhanced absorption spectroscopy by diode-laser self-locking," Appl. Phys. B **80**, 1027-1038 (2005).
34. B. Lance, G. Blanquet, J. Walrad, and J.-P. Bouanich, "On the speed-dependent hard collision lineshape models: Application to C_2H_2 perturbed by Xe," J. Mol. Spectrosc. **185**, 262-271 (1997).
35. S. Wójtewicz, K. Stec, P. Masłowski, A. Cygan, D. Lisak, R. S. Trawiński, and R. Ciuryło, "Low pressure lineshape study of self-broadened CO transitions in the $(3 \leftarrow 0)$ band," J. Quant. Spectrosc. Radiat. Transfer **130**, 191-200 (2013).
36. A. Cygan, D. Lisak, S. Wójtewicz, J. Domysławska, J. T. Hodges, R. S. Trawiński, and R. Ciuryło, "High-signal-to-noise-ratio laser technique for accurate measurements of spectral line parameters," Phys. Rev. A **85**, 022508 (2012).

#237196 - $15.00 USD Received 31 Mar 2015; revised 6 May 2015; accepted 11 May 2015; published 22 May 2015

37. A. Cygan, D. Lisak, P. Masłowski, K. Bielska, S. Wójtewicz, J. Domysławska, R. S. Trawiński, R. Ciuryło, H. Abe, and J. T. Hodges, "Pound-Drever-Hall-locked, frequency-stabilized cavity ring-down spectrometer," Rev. Sci. Instrum. **82**, 063107 (2011).
38. J. Y. Wang, P. Ehlers, I. Silander, and O. Axner, "Dicke narrowing in the dispersion mode of detection ad in noise-immune cavity-enhanced optical heterodyne molecular spectroscopy - theory and experimental verification," J. Opt. Soc. Am. B **28**, 2390-2401 (2011).
39. N. C. Wong, and J. L. Hall, "Servo control of amplitude modulation in frequency-modulation spectroscopy: demonstration of shot-noise-limited detection," J. Opt. Soc. Am. B **2**, 1527-1533 (1985).
40. A. Cygan, D. Lisak, S. Wójtewicz, J. Domysławska, R. S. Trawiński, and R. Ciuryło, "Active control of the Pound-Drever-Hall error signal offset in high-repetition-rate cavity ring-down spectroscopy," Meas. Sci. Technol. **22**, 115303 (2011).
41. J. Y. Wang, P. Ehlers, I. Silander, J. Westberg, and O. Axner, "Speed-dependent Voigt dispersion line-shape function: applicable to techniques measuring dispersion signals," J. Opt. Soc. Am. B **29**, 2971-2979 (2012).
42. L. Galatry, "Simultaneous effect of Doppler and foreign gas broadenig on spectral lines," Phys. Rev. **122**, 1218 (1961).
43. M. Izutsu, S. Shikama, and T. Sueta, "Integrated optical SSB modulator/frequency shifter," IEEE J. Quantum Electron. **QE-17**, 2225-2227 (1981).
44. S. A. Diddams, D. J. Jones, J. Ye, S. T. Cundiff, J. L. Hall, J. K. Ranka, R. S. Windeler, R. Holzwarth, T. Udem, and T. W. Hänsch, "Direct link between microwave and optical frequencies with a 300 THz femtosecond laser comb," Phys. Rev. Lett. **22**, 5102 (2000).
45. R. Holzwarth, T. Udem, T. W. Hänsch, J. C. Knight, W. J. Wadsworth, and P. St. J. Russell, "Optical frequency synthesizer for precision spectroscopy," Phys. Rev. Lett. **85**, 2264 (2000).
46. T. Sakamoto, T. Kawanishi, and M. Izutsu, "Widely wavelength-tunable ultra-flat frequency comb generation using conventional dual-drive Mach-Zehnder modulator," Electron. Lett. **43**, 1039-1040 (2007).
47. D. A. Long, A. J. Fleisher, K. O. Douglass, S. E. Maxwell, K. Bielska, J. T. Hodges, and D. F. Plusquellic, "Multiheterodyne spectroscopy with optical frequency combs generated from a continuous-wave laser," Opt. Lett. **39**, 2688-2690 (2014).
48. D. A. Long, A. J. Fleisher, S. Wójtewicz, and J. T. Hodges, "Quantum-noise-limited cavity ring-down spectroscopy," Appl. Phys. B **115**, 149-153 (2014).
49. T. Day, E. K. Gustafson, and R. L. Byer, "Sub-hertz relative frequency stabilization of two-diode laser-pumped Nd:YAG lasers locked to a Fabry-Perot interferometer," IEEE J. Quantum Electron. **28**, 1106-1117 (1992).
50. K. Numata, A. Kemery, and J. Camp, "Thermal-noise limit in the frequency stabilization of lasers with rigid cavities," Phys. Rev. Lett. **93**, 250602 (2004).
51. A. Foltynowicz, P. Masłowski, A. J. Fleisher, B. J. Bjork, and J. Ye, "Cavity-enhanced optical frequency comb spectroscopy in the mid-infrared application to trace detection of hydrogen peroxide," Appl. Phys. B **110**, 163-175 (2013).
52. M. J. Thorpe, R. J. Jones, K. D. Moll, J. Ye, and R. Lalezari, "Precise measurements of optical cavity dispersion and mirror coating properties via femtosecond combs," Opt. Express **13**, 882-888 (2005).

1. Introduction

Spectroscopy is a powerful measurement tool that can provide deep insight into the physics governing the microscopic world. Studies of the internal structure of atoms [1] or fundamental molecular interactions [2] are representative and scientifically important investigations which rely upon advanced spectroscopic measurements. Another challenge is the precise metrology of gaseous concentration and its composition necessary for remote sensing of the atmosphere [3] and for monitoring climate change [4]. High-accuracy spectroscopy plays also a vital role in the determination of physical constants [5] and in tests of their stability [6].

An electromagnetic wave propagating in an absorbing medium experiences attenuation of its amplitude and shift of its phase. These mechanisms, which are ascribed to absorption and dispersion respectively, are interrelated in case of linear response limit by the familiar Kramers-Krönig equations [7]. Although both effects can be used to quantify the amount of substance, absorption measurements are more common than those of phase, which are generally more experimentally demanding. In the vicinity of an absorbing (amplifying) medium placed inside a high-finesse optical cavity, absorption and dispersion effects cause characteristic cavity mode broadening (narrowing) and pushing (pulling) relative to the absorption peak.

The first demonstration of absorptive broadening of cavity modes was reported by Nakagawa

#237196 - $15.00 USD Received 31 Mar 2015; revised 6 May 2015; accepted 11 May 2015; published 22 May 2015

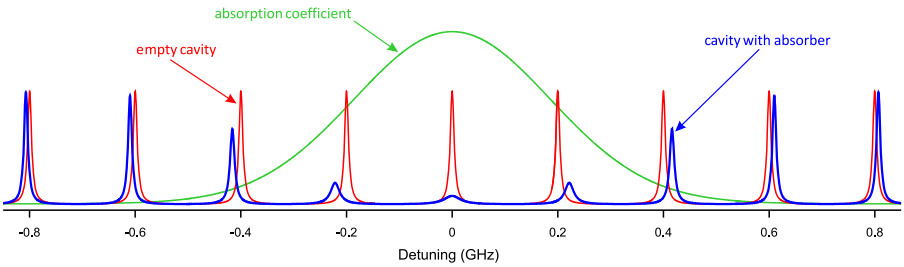

Fig. 1. The comb of cavity modes in the presence and absence of intracavity medium. The spectral broadening and frequency pushing of cavity modes caused by absorption and dispersion phenomena is illustrated. These two effects are measured by the CMWS and 1D-CMDS techniques, respectively.

et al. [8]. A key spectroscopic application of this phenomena relies on the laser linewidth narrowing technique [9]. It was shown recently that by using an ultra-narrow laser [10, 11] or the frequency-agile, rapid scanning (FARS) spectroscopy [12, 13] method, transmission spectra of high-finesse cavity modes, which are insensitive to the instrumental function can be obtained. This motivated development of cavity mode-width spectroscopy (CMWS): a new experimental technique which is complementary to the well-known cavity ring-down spectroscopy (CRDS) in the high absorption range where ring-down decays are too short for accurate measurements [11, 13].

The effect of pulling and pushing of mode frequencies was addressed in many works in laser technology [14, 15, 16]. However, its application to laser spectroscopy is mostly limited to frequency modulation (FM) techniques [17, 18]. In those studies phase modulation of the laser light provides an unbalanced heterodyne beat signal at the modulation frequency when the spectral feature is probed. A high sensitivity of both absorption and dispersion detection modes can be increased even down to the shot-noise limit by the use of high-finesse cavities as in the NICE-OHMS method [19]. However, the accuracy of FM spectroscopy as well as all methods based on the measurement of light intensity is usually limited by instrumental errors of the detection system and detection phase uncertainty.

Frequency-based measurements of dispersion spectra have been previously suggested by Nakagawa *et al.* [8] as a way to improve sensitivity. The proof-of-concept experiment was supposed to rely on measuring the variation in heterodyne beat frequency between two lasers locked to different dispersion-pushed cavity modes. Although the idea was brilliant, no experiment confirming this method was carried out. Another approach to the measurement of dispersion spectra is differential intracavity phase spectroscopy, introduced by Diddams *et al.* [20]. This technique is based on measuring the relative phase shifts between two counterpropagating fields in a ring laser with an absorbing intracavity medium. Although absorption sensitivities achieved by this technique are relatively high, they are still several orders of magnitude worse than those obtained in cavity-enhanced absorption spectroscopy (CEAS).

In this Article we demonstrate the novel one-dimensional cavity-mode dispersion spectroscopy (1D-CMDS) and its potential in application to gas metrology, line-shape studies as well as in fundamental physics. Here, ”one-dimensional” means that only a frequency-domain-measured quantity, namely the frequency of cavity modes, is used to quantify dispersion spectra. The proposed method combines the current need for high-accuracy spectroscopic studies [21] with the best recent achievements in optical frequency control [22, 23]. Some preliminary results of the cavity mode dispersion measurements were recently reported [24, 25]. A general formula for the dispersion profile extending the discussion in [26, 27] is given here for an

#237196 - $15.00 USD Received 31 Mar 2015; revised 6 May 2015; accepted 11 May 2015; published 22 May 2015

arbitrary line-shape model.

This study expands previous works on dispersion spectroscopy [20, 26] with respect to both detection sensitivity as well as spectral accuracy. The former is substantially increased in CEAS techniques and is limited only by the quality of the laser-to-cavity lock and by the stability of the frequency comb of cavity modes. The latter can be potentially high, because of the negligible influence of the detection system on the measured cavity mode positions and the ability to tightly lock the laser to the cavity mode. Although our experimental setup is relatively simple, it allows for high-precision and concurrent measurements of spectra by three independent techniques: conventional time-based CRDS, as well as frequency-based CMWS and 1D-CMDS. These complementary approaches can be directly compared to quantify and bound the respective systematic errors. It is expected that such comparisons will provide a crucial test toward the development of ultra-high-accuracy spectroscopy.

2. Theory

The time constant τ of the light intensity decay from the cavity, measured in a CRDS experiment, can be considered as the average intracavity photon lifetime. Because the cavity mode width (full width at half maximum - FWHM) $\delta\nu_m$ and τ form a Fourier-transform pair, it follows that $\delta\nu_m = 1/(2\pi\tau)$. The cavity mode shape describes the spectral energy distribution of standing waves propagating in the cavity, which for a high-finesse cavity can be well approximated by the Lorentzian line-shape function [11]. Intuitively, shortening of the photon lifetime caused by the intracavity absorption results in broadening of cavity modes. In addition, an intracavity phase shift of the light changes the resonance conditions for the standing waves. This phase shift is manifested as a frequency pushing of the cavity modes away from the local absorption resonance. Both phenomena are illustrated in Fig. 1.

Near the absorption resonance, the complex refractive index $n_a(\nu) = n + n'(\nu) - i\kappa(\nu)$ depends on frequency ν. It includes the resonant component $n'(\nu) - i\kappa(\nu)$ and the real nonresonant component n. A general formula describing the intensity transmission through a medium bounded by a two-mirror cavity is given by [11, 28]

$$\mathscr{T}(\nu) = \frac{T^2 \mathrm{e}^{-\alpha(\nu)\ell}}{(1 - R\mathrm{e}^{-\alpha(\nu)\ell})^2 + 4R\mathrm{e}^{-\alpha(\nu)\ell}\sin^2[\pi\nu/\xi(\nu)]}, \tag{1}$$

where T and R are, respectively, the intensity transmission and reflectivity of the cavity mirrors, $\alpha(\nu)$ is the frequency-dependent absorption coefficient and ℓ is the cavity length. For integer values of the ratio $\nu/\xi(\nu)$, this function exhibits maxima that correspond to resonant frequencies ν_N which can be found by solving the equation $\nu_N = N\xi(\nu_N)$, where N is the integer mode order. Here $\xi(\nu)$ is a frequency-dependent quantity related to the free spectral range (FSR) of the unperturbed cavity modes.

The FSR is given by ν_{FSR}=$c/(2n\ell)$ and corresponds to the mode spacing in the absence of resonant absorption. In general, $\alpha(\nu)$ and $\xi(\nu)$ are related to the absorptive and dispersive parts of $n_a(\nu)$ by $\alpha(\nu) = 2k_0\kappa(\nu)$ and $\xi(\nu) = \nu_{\mathrm{FSR}}/(1 + n'(\nu)/n)$, where $k_0 = 2\pi\nu_0/c$ is the wave vector corresponding to the transition frequency ν_0 and c is the speed of light. In the absence of absorption, Eq. (1) reduces to the well-known Airy equation, and the mode frequencies are equally spaced and given by ν_N= $N\nu_{\mathrm{FSR}}$.

The quantities $n'(\nu)$ and $\kappa(\nu)$ are related by the common Kramers-Krönig relations [7]. For an arbitrary line-shape model, these terms can be expressed as the imaginary and real parts of the complex line-shape function $\mathscr{I}(\nu)$:

$$n'(\nu) = c\mathscr{N}S\,\frac{-\mathrm{Im}[\mathscr{I}(\nu - \nu_0)]}{2k_0}, \tag{2}$$

#237196 - $15.00 USD Received 31 Mar 2015; revised 6 May 2015; accepted 11 May 2015; published 22 May 2015

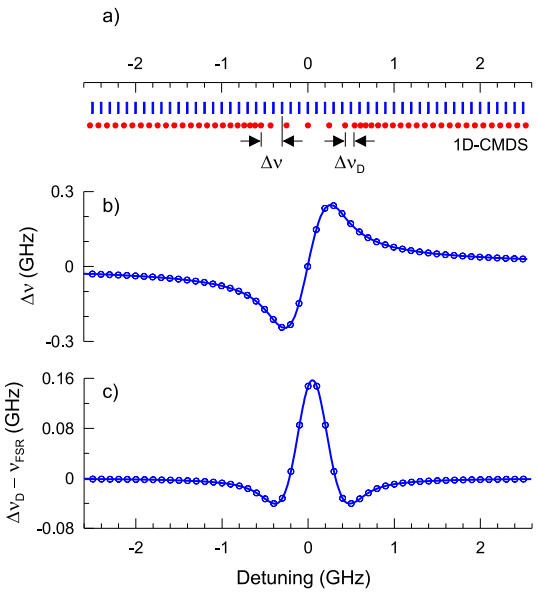

Fig. 2. One-dimensional CMDS. (a) The combs of cavity modes in the vicinity (dots) and absence (sticks) of the intracavity medium form one-dimensional dispersion spectra solely in the frequency domain. In the absorption case clear frequency-pushing of the cavity modes caused by dispersion is shown. (b) The original 1D-CMDS spectrum transformed to a two-dimensional spectrum based on the frequency differences $\Delta\nu$ between the dispersion-perturbed (dots in panel a) and unperturbed (sticks in panel a) cavity modes of the same order. (c) The original 1D-CMDS spectrum transformed to a differential two-dimensional spectrum based on the frequency intervals $\Delta\nu_D$ calculated in terms of the centers of the $(N+k)$-th and the N-th dispersion-perturbed cavity modes and given by Eq. (4). In these simulations, $k=1$ and the FSR of the empty cavity was $\nu_{\mathrm{FSR}}=0.1$ GHz. For clarity, the dispersive shift of the cavity modes $\Delta\nu$ was scaled by a factor of 5×10^4.

$$\kappa(\nu)=c\mathscr{N}S\,\frac{\mathrm{Re}[\mathscr{I}(\nu-\nu_0)]}{2k_0}. \tag{3}$$

In the above equations $\mathscr{N}$ and S are the number density of the absorber and the line intensity, respectively. The line-shape function $\mathscr{I}(\nu)$ is normalized to unity, i.e. $\int\mathscr{I}(\nu)d\nu=1$, and may take various forms depending on the line-shape effects that are taken into account [29]. This complex line shape can be also viewed as a quantity related to the Fourier transform of the medium response function to the incident electromagnetic field which causality leads to the Kramers-Krönig relations [30].

The 1D-CMDS method presented here relies on the measurement of cavity mode frequencies that are affected by the intracavity medium, see Fig. 2a. The lower panels b) and c) in Fig. 2 present mappings of 1D-CMDS spectra onto traditional two-dimensional spectra. They represent two different realizations of 1D-CMDS called here "direct" and "differential", respectively. It should be emphasized that frequency - the physical quantity that can be measured the best [31], appears on both the horizontal and vertical axes. In the case of differential 1D-CMDS, the frequency intervals $\Delta\nu_D$ between centers of the $(N+k)$-th and N-th longitudinal cavity modes are given by the implicit relation

$$\Delta\nu_D(k)=(N+k)\xi(\nu_L+\Delta\nu_D(k))-N\xi(\nu_L), \tag{4}$$

#237196 - $15.00 USD Received 31 Mar 2015; revised 6 May 2015; accepted 11 May 2015; published 22 May 2015

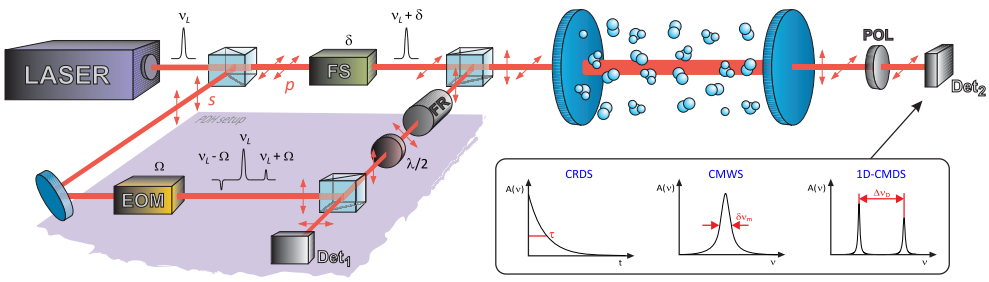

Fig. 3. Scheme of the experiment. Laser light with initial frequency ν_L is split into probing (p-polarized) and locking (s-polarized) beams. A tight lock of the laser frequency to a cavity mode is realized by the Pound-Drever-Hall technique with the laser light phase modulated at RF frequency Ω by an electrooptic modulator (EOM). A half-wave plate ($\lambda/2$) and a Faraday rotator (FR) are used to redirect the interfering light from the cavity to a detector Det_1 to produce an error signal for the locking servo. The frequency shifter (FS) is an acousto-optic modulator which detunes the probe beam frequency by δ from the locking frequency ν_L to enable scanning across the cavity mode. The transmitted probe beam intensity is measured by detector Det_2, and the locking beam is blocked by the polarizer (Pol). The cavity length is actively stabilized to the reference laser (not shown in the scheme) by a method described in Ref. [32]. Three alternative techniques, CRDS, CMWS and 1D-CMDS can be realized with this setup.

where ν_L is the frequency of the laser locked to the N-th cavity mode and $\nu_L + \Delta\nu_D(k)$ is the frequency of the probe beam shifted by k longitudinal cavity modes from the locking beam (for $k = 1$ $\Delta\nu_D(k) = \Delta\nu_D$). To explicitly show the dispersive character of $\xi(\nu)$, resulting from Eq. (2), we can write it as

$$\xi(\nu) = \frac{\nu_{\mathrm{FSR}}}{1 - c\mathcal{N}S\,\mathrm{Im}[\mathcal{I}(\nu - \nu_0)]/(2nk_0)}. \tag{5}$$

Equations (4) and (5) can be combined to model the spectral dependence of $\Delta\nu_D$. Modeled spectra are determined by least-squares fits of these equations to the measured $\Delta\nu_D$ in which the number density and line parameters can be treated as adjustable quantities.

3. Experiment

The precise measurements of the shapes and positions of cavity modes requires spectrally narrow lasers (relative to the cavity mode width) and the use of length-stabilized cavities. To achieve the former condition, a convenient approach is to implement a two-beam scheme in which the laser is tightly locked to the cavity. In this configuration, a part of the beam (which is frequency-detuned from the laser beam that is locked to one of the cavity modes) is insensitive to cavity length variations caused by vibrations and thermal drift. Hence, this component can be used successfully to probe the cavity mode shapes with the high precision. Such a solution is in contrast with that discussed in [11] where the laser and cavity were treated as two independent systems. It should be noted that currently available technology allows for relative locking of the laser and cavity at the level of tens of mHz [22, 23]. Moreover, an active stabilization of the cavity length to the external laser [32] prevents thermal drift of the comb of cavity modes.

A brief summary of the proof-of-principle experiment is given (see Fig. 3 for this scheme). For clarity, all technical details are provided by the Section labeled “Methods”. The laser beam at frequency ν_L is polarization split into two legs. The s polarization is used to tightly lock the laser to the cavity mode. We use for this purpose the Pound-Drever-Hall (PDH) scheme [9],

#237196 - $15.00 USD Received 31 Mar 2015; revised 6 May 2015; accepted 11 May 2015; published 22 May 2015

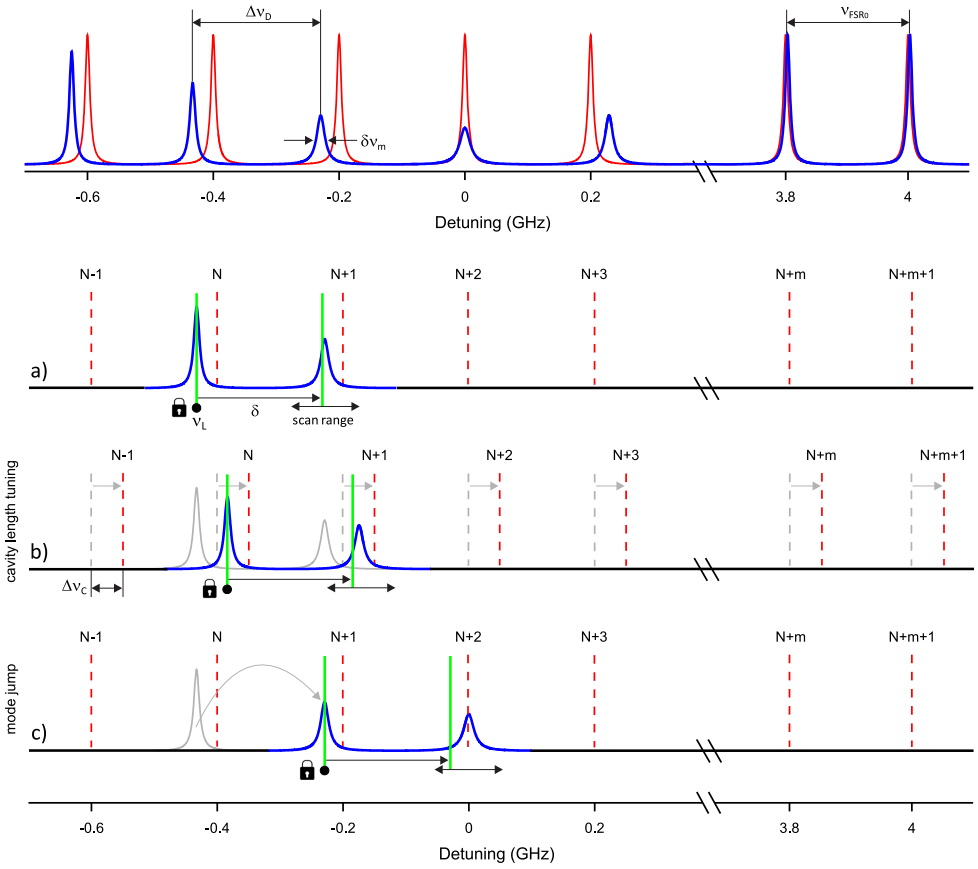

Fig. 4. Principle of the 1D-CMDS method. (a) The δ-detuned part of the beam of the laser locked to the N-th cavity mode is scanned across the $(N+1)$-th mode to record its shape. The information about the intracavity differential dispersion between the $(N+1)$-th and N-th cavity modes is retrieved from the frequency interval $\Delta\nu_D$ between peak of the $(N+1)$-th mode and the locking point frequency ν_L at the N-th mode. Absorption information is obtained from the width $\delta\nu_m$ of the $(N+1)$-th cavity mode profile. (b) The density of spectral points can be increased by measuring the differential dispersion between cavity modes shifted by $\Delta\nu_c$ as a result of controlled changes in the cavity length. (c) After successful measurement of the differential dispersion between the N-th and $(N+1)$-th modes, the laser is relocked to the next $(N+1)$-th mode and another frequency interval between the $(N+2)$-th and $(N+1)$-th modes is measured.

#237196 - $15.00 USD Received 31 Mar 2015; revised 6 May 2015; accepted 11 May 2015; published 22 May 2015

but the optical feedback method [33] can be used as well. The *p*-polarized beam detuned by δ from the laser locking point is scanned in small steps around another cavity mode to measure its shape (Fig. 4a). Because of the intracavity medium the cavity modes are broadened and frequency-pushed relative to the absorption profile center. To record the dispersion as well as the absorption spectrum, the frequency of the locking laser (*s*-polarized) is stepped in increments of the cavity FSR. After each mode jump, the laser is relocked to the nearest cavity mode and the next cavity mode shape is measured by scanning the *p*-polarized beam (Fig. 4c). The determined positions of the cavity modes designate subsequent frequency intervals $\Delta\nu_D$ between the cavity modes defined by Eq. (4). These frequency intervals give the 1D-CMDS dispersion spectrum in a differential realization. Additionally, the measured spectral widths $\delta\nu_m$ of cavity modes yield the CMWS spectrum. Finally, the CRDS spectrum is obtained from the set of measured time constants τ for the light decays obtained after rapidly switching off the *p*-polarized beam.

In our experiment spectra also can be measured with frequency steps which are smaller than the cavity FSR. This is possible because the cavity length can be changed in a controlled way by frequency tuning of an external laser to which the cavity is locked. This causes a frequency shift of the cavity mode comb (Fig. 4b) which near the frequency ν_L is well approximated by $\Delta\nu_C = \nu_L\Delta\nu_{\mathrm{FSR}}/\nu_{\mathrm{FSR}}$, where $\Delta\nu_{\mathrm{FSR}}/\nu_{\mathrm{FSR}}$ is the relative change of the cavity FSR far from the absorption line. The natural limit of cavity length tuning precision is the stability of the reference laser.

4. Results

The performance of our spectrometer was illustrated by measuring the $(3 \leftarrow 0)$ band $^{13}C^{16}O$ P3 transition ($\tilde{\nu}_0 = 6200.9964\ \mathrm{cm}^{-1}$) using the three alternative methods: CRDS, CMWS and 1D-CMDS. The corresponding residuals from fits of the Voigt profile (VP) and the more sophisticated speed-dependent Nelkin-Ghatak profile (SDNGP) [34] are presented below each spectrum (see Fig. 7). The line shape of this transition was carefully studied before [35].

An example of the measured cavity mode shape and the corresponding residuals, i.e. differences between the experimental profile and fitted line-shape model (Lorentzian in this case) are shown in Fig. 5. It demonstrates the sub-Hz precision of measurements of the cavity mode widths and the position resolution achieved in our experiment. Indeed, the measured cavity mode width of 1.45 kHz (cavity finesse of 141500) has an uncertainty of approximately 330 mHz whereas measurement uncertainty in the mode position is more than threefold smaller. These uncertainties are result of an achieved quality of the fit factor QF = 995 for the cavity mode shape measurement (calculated as a ratio of the cavity mode peak to the standard deviation of fit residuals [36]) and the number of 1000 points used per recorded spectrum, see Fig. 5. We found that the main contribution to the statistical noise of the cavity mode width and position comes from the quality of the lock between the laser and cavity. This frequency noise is confirmed by the characteristic shape of residuals, i.e. the largest noise amplitude occurs at the greatest derivative of the cavity mode profile. Also, the frequency noise introduced by the acousto-optic modulator, which was used in our experiment as a frequency shifter for the probe beam, was negligible because the driving RF signal was stabilized with respect to a GPS-referenced Rb frequency standard.

For the absorption and dispersion spectra shown in Fig. 7, we measured the frequency fluctuations of the laser relative to the cavity mode center to be 50 Hz. We estimated this quantity for non-absorption conditions from the statistical distribution of measured frequency differences between cavity modes based on a 1 s averaging time. These frequency intervals were then used in an Allan variance analysis to calculate the lower limit of the frequency noise affecting measurements of cavity mode positions (see Fig. 6). The achieved limit of 1.4 Hz corresponds to a slow drift of the locking point in the Pound-Drever-Hall method (that affects a drift of $\Delta\nu_D$

#237196 - $15.00 USD Received 31 Mar 2015; revised 6 May 2015; accepted 11 May 2015; published 22 May 2015

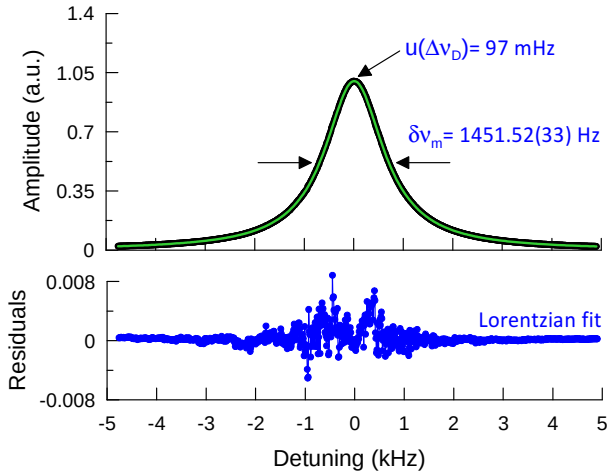

Fig. 5. Precision of the cavity mode width and position measurement. Shape of a single cavity mode recorded at non-absorption conditions and residuals from a Lorentzian profile fit. The statistical standard uncertainties of the cavity mode width and position determined from fitting the spectra are $u(\delta\nu_m) = 330$ mHz and $u(\Delta\nu_D) = 97$ mHz, respectively.

frequency intervals) and slow cavity FSR variations that result from the long-term instability (2 MHz/h) of the reference laser used for the cavity length control. Here we have demonstrated a minimum detectable absorption of 6.4×10^{-10} cm^{-1}, which is comparable to sensitivities achieved with other CRDS techniques [13, 37]

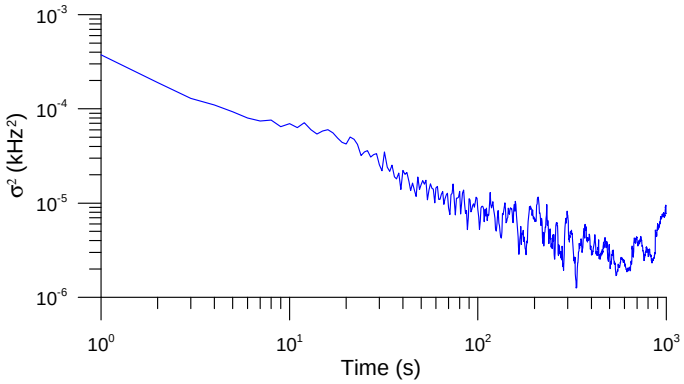

Fig. 6. Allan variance plot of frequency intervals $\Delta\nu_D$. The minimum corresponds to the 1.4 Hz-frequency noise limit in cavity mode position measurements.

The quality of the fit factor QF [36] of 1639 obtained for the 1D-CMDS spectrum is to our knowledge the highest so far obtained for any dispersion method. This level of precision enabled us to implement a rigorous line-shape analysis. To this end we used various theoretical models starting from the VP and more advanced profiles including the SDNGP which goes beyond the VP by taking into account two subtle line-narrowing effects - Dicke narrowing and the speed dependence of collisional broadening. So far a dispersive line-shape analysis has been carried out only for NICE-OHMS acetylene spectra [26, 38]. However, unlike the 1D-CMDS, the NICE-OHMS method is based on light intensity measurements.

In Fig. 7 we compare three CO spectra obtained with the respective spectroscopic techniques

#237196 - $15.00 USD Received 31 Mar 2015; revised 6 May 2015; accepted 11 May 2015; published 22 May 2015

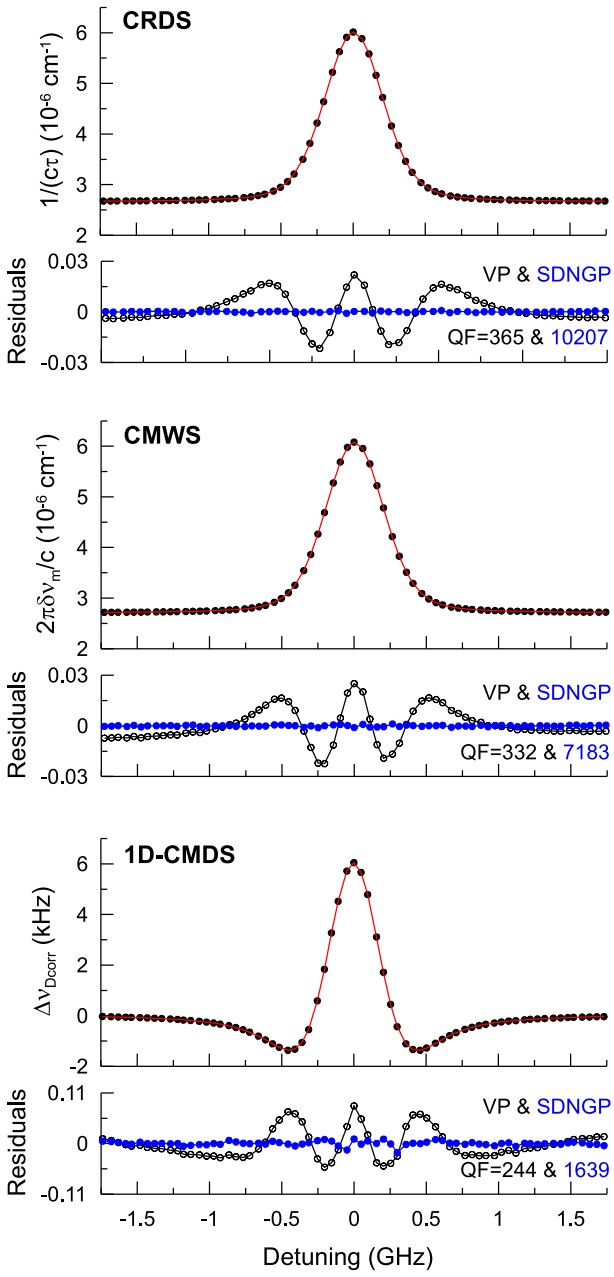

Fig. 7. Alternative approaches to cavity-enhanced spectroscopy. Experimental (dots) and fitted (line) spectrum of the $^{13}C^{16}O$ P3 transition from the $(3 \leftarrow 0)$ band recorded at a pressure of 2.9 kPa by three independent techniques: CRDS, CMWS and 1D-CMDS. Below are residuals from fits with the Voigt profile (VP) - open circles and the more general speed-dependent Nelkin-Ghatak profile (SDNGP) - dots. Each of the presented spectra is a result of 65 scans averaging. The CRDS and CMWS methods provide the absorption spectrum, whereas the 1D-CMDS spectrum is dispersive and differential because it measures frequency intervals between cavity modes. In all cases, the SDNGP properly matches the experimental data. Note that the y-axis label $\Delta\nu_{\mathrm{Dcorr}}$ is defined below in the Section labeled "Methods".

#237196 - $15.00 USD Received 31 Mar 2015; revised 6 May 2015; accepted 11 May 2015; published 22 May 2015

discussed here. All measurements undoubtedly indicate that the SDNGP properly reproduces the measured spectra. However, discrepancies between the fitted line-shape parameters obtained by these methods are much greater than the measurement uncertainties reported by the fitting algorithm. We found an agreement of 0.6% with fitted line area and collisional width determined by CRDS and CMWS techniques. For the 1D-CMDS method we found that these two parameters can differ from CRDS results by 4% and 7.5%, respectively. This discrepancy occurs when the frequency interval, $\Delta\nu_D$, between cavity modes is measured relative to the laser-to-cavity locking point: a measurement that is affected by the temporal drift of a DC offset in the laser locking feedback loop [39, 40]. This effect shifts the locked laser frequency away from the cavity mode center and introduces error into the measured mode-to-mode frequency intervals. The magnitude of this perturbation is especially sensitive to the absorption, and consequently, as the laser lock is moved from mode to mode, different frequency shifts of the locking point cause distortion of the measured dispersion profile. We found that this problem can be overcome at the sub-Hz level of precision when the frequency interval between two cavity mode centers is measured on the opposite sides of the locking point. We realized this method using two acousto-optic modulators which were symmetrically detuned by one cavity FSR, up and down from the locking point frequency. This arrangement enables the simultaneous measurement of two cavity mode positions, yielding agreement of 1.3% and 3.3% between the CRDS and 1D-CMDS determinations of line area and collisional width, respectively. These results for dispersive and absorptive spectra are in better agreement than those recently reported by Wang et al. [26, 27, 41] using NICE-OHMS. Indeed, an exact agreement between line areas and collisional widths obtained from these two types of spectra should not be expected at this point. First, as was demonstrated by Wang et al. [26, 27, 41] fits to dispersion spectra are highly sensitive to the choice of line-shape model, where it was shown that percent-level discrepancies between line intensities, collisional width and narrowing parameters can be obtained between absorption and dispersion profiles. Second, the sensitivity of the dispersion method to the line-shape model is even stronger for differential measurement techniques applied to the 1D-CMDS method. We performed simulations of the 1D-CMDS and absorption spectra at our experimental conditions using two different line-shape models. To this end, we used a Galatry profile [42] that was fit to the SDNGP [34] chosen as a reference profile. Consistent with our observations, for the differential dispersion measurements the analysis resulted in differences between the fitted line areas and collisional widths of 0.6% and 4.2%, respectively, whereas we calculated discrepancies of 0.2% and 0.8% for the common absorption case. Finally, sub-percent differences between CRDS and two other techniques can be assigned to limitations resulting from nonlinearities in the ring-down signal detection system. On the other hand, the insensitivity to nonlinearities in the detection system as well as the purely frequency domain nature of the spectral measurements underscore the main advantages of the 1D-CMDS method and indicate its potential for advanced spectroscopic applications.

The 1D-CMDS technique presented here has several logical extensions and improvements. For example, higher-bandwidth devices such as broadly tunable offset-locked lasers [11], high-bandwidth electro-optic modulators [12, 13] or Mach-Zehnder single-sideband modulators [43] can be used as frequency shifters for the probe beam. Such solutions assure a higher tuning range of the probe beam as well as a more stable, unperturbed reference beam during dispersion because of its location far from the absorption line. In the case where the spectrum acquisition rate is important, optical frequency combs based on mode-locked lasers [44, 45] and continuous-wave lasers [46, 47] can be used in the 1D-CMDS to simultaneously probe all frequency intervals between cavity modes within the absorption profile. In this way, temporal drifts of physical quantities can be minimized as well.

Further improvement of the 1D-CMDS sensitivity even by two orders of magnitude is

#237196 - $15.00 USD Received 31 Mar 2015; revised 6 May 2015; accepted 11 May 2015; published 22 May 2015

promising and achievable. Crucial to this level of performance would be a sub-Hz-level relative lock between the laser and cavity [22], control of the cavity mode comb referenced to a laser having a stability at least several tens of kHz as well as acoustic isolation of the cavity and the use of Cs frequency standards or optical atomic clocks for stabilization of the RF signals. Because the cavity mode profile has to be scanned to find its center, its determination can be perturbed by amplitude noise of the probe laser. Heterodyne detection of the cavity mode profiles enables one to suppress the amplitude noise according to the $1/f$ dependence [48] and to approach the quantum noise limit imposed by photons themselves. The shot noise also sets the lowest limit to which the laser linewidth can be narrowed as well as limits the performance of the PDH locking method [49]. Another fundamental limit of 1D-CMDS sensitivity is set by the thermal noise (Brownian motion) of the cavity mirror substrates [50] that designate the boundaries of the cavity FSR stability.

It should be noted that theory and results of 1D-CMDS technique presented in this work do not take into account dispersion of cavity modes introduced by multilayer dielectric coatings of the cavity mirrors. The nonlinearity of this dispersion grows as one moves from the center of the mirror coating band and in case of broad-band measurements [51] leads to even tens of kHz shifts in cavity modes. Similar problem of nonlinear background level of the spectrum occurs in all cavity enhanced spectroscopic methods. However, in case of short-range (several tens of GHz) scans through the dispersion resonance this effect provides mainly a linear, systematic shift of all cavity modes within the scanning range and thus its possible influence on the dispersion line shape can be neglected. Moreover, the quantities $n'(\nu)$ and $\kappa(\nu)$ given by Eqs. (2) and (3) are related by the Kramers-Krönig equations which are valid only for the linear limit of absorption. This means that any saturation effects occurring in the cavity and not taken into account in the analysis of both absorption and dispersion line shapes can limit the accuracy of such measurements. It should be noted that in case of CRDS, CMWS and 1D-CMDS experiments discussed here we did not observe, at the given level of precision, any systematic distortions of ring-down signals, cavity mode profiles and irregularities in the cavity mode shifts which could suggest the presence of nonlinear saturation effects.

5. Methods

The probe/lock laser used in the experiment shown in Fig. 3 is an external cavity diode laser (*New Focus*, model TLB-6330). Its mode-hop free tuning range and free-running linewidth are 1550-1630 nm and 300 kHz, respectively. A typical output power is 15 mW. The Pound-Drever-Hall method used to frequency stabilize the laser to the optical cavity mode enables narrowing of its linewidth by more than three orders of magnitude. The optical cavity filled with probing gas is formed by two double-coated, spherical, super-polished mirrors. We used in the experiment two sets of mirrors (*Layertec GmbH*) having reflectivities of 99.995% and 99.98% for 1570 nm, and 98% for 633 nm. The frequency stabilized HeNe laser (*Melles Griot*) with stability of 2 MHz/h was used to actively stabilize the comb of the cavity modes by the method described in [32].

The dispersion spectrum presented in Fig. 7 was acquired in frequency steps of the cavity FSR equal to $\nu_{\mathrm{FSR}} \approx 204$ MHz with four cavity length tuning points causing mode shifts of $\Delta\nu_C \approx 0, 50, 100, 150$ MHz, respectively. Such a spectrum has a background level that is dependent on the cavity length, see the upper spectrum in Fig. 8. To focus only on the intracavity dispersion effects, the real experimental spectrum given by Eq. (4) was shifted by the absolute value of the frequency interval $k\nu_{\mathrm{FSR}}$, measured between k consecutive cavity modes far from the absorption transition, and corrected by the change of the cavity FSR caused by the cavity

#237196 - $15.00 USD Received 31 Mar 2015; revised 6 May 2015; accepted 11 May 2015; published 22 May 2015

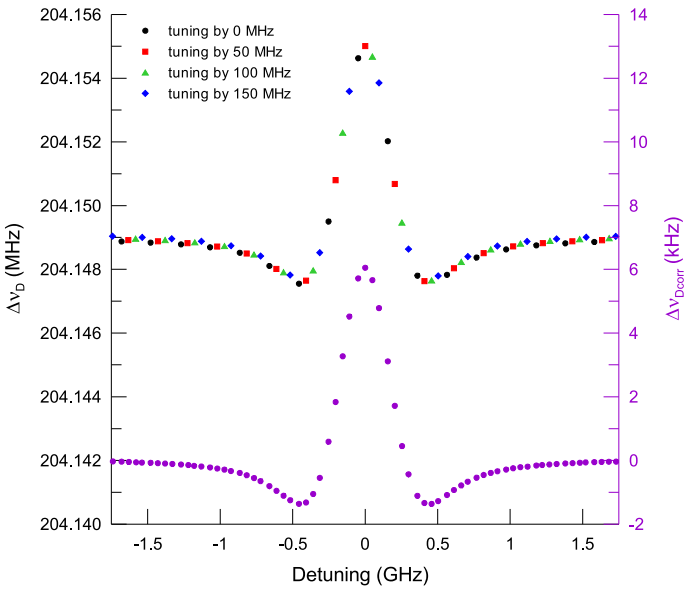

Fig. 8. Treatment of the 1D-CMDS spectrum. The experimental spectrum (see upper graph and left axis) obtained by 1D-CMDS has a background level that depends on the cavity length. Especially, when the cavity length is tuned during acquisition process, characteristic oscillations appear on the recorded profile. They correspond to slightly different values of the cavity FSR marked by different colors. To focus only on the dispersive character of the spectrum, the background is subtracted from the experimental data (see lower graph and right axis) according to Eq. (6) with $k = 1$. This form of the 1D-CMDS spectrum is a subject for further analysis.

length tuning $k\Delta\nu_C/N$ according to relation:

$$\Delta\nu_{\mathrm{Dcorr}}(k) = \Delta\nu_D(k) - k\frac{\Delta\nu_C}{N} - k\nu_{\mathrm{FSR}}. \tag{6}$$

A graphical comparison of the real $\Delta\nu_D(k)$ and corrected $\Delta\nu_{\mathrm{Dcorr}}(k)$ dispersion spectra is presented in Fig. 8.

6. Conclusions

To conclude, we have demonstrated the idea of a new dispersion spectroscopy technique entirely based on frequency measurements. An important result is that this presently is the only spectroscopy technique which is one-dimensional. It needs only one physical quantity, i.e. the frequencies of cavity mode centers, to provide full information about the spectrum. The tremendous potential of this technique results from the combination of recent achievements in absolute frequency measurements and from the development of advanced laser frequency stabilization methods driven by contemporary needs for high-precision and high-accuracy spectroscopy. In contrast to common intensity-based methods (even frequency-based), our method is insensitive to instrumental errors of the detection system which are particularly important to accurate line-shape studies. We demonstrated the highest so far precision that was achieved for any measured dispersion spectra. This level of precision enabled the rigorous line-shape analysis of a CO spectrum with the use of more complex theoretical models than the common Voigt profile. Moreover, we expect that this approach can be used for rigorous tests of the Kramers-Krönig

#237196 - $15.00 USD Received 31 Mar 2015; revised 6 May 2015; accepted 11 May 2015; published 22 May 2015

relations at the sub-percent level. We also expect that this technique will enable ultra-precise measurements of dispersion and optical properties of high-reflectivity mirror coatings. Such measurements should provide new capabilities for characterizing material non-linearities which are relevant to optical cavities used for pulse energy enhancement, high-harmonic generation and broadband comb-based spectroscopy [52]. Finally, we describe how to extend our method and to improve its sensitivity to best exploit the potential of modern optical systems.

Acknowledgments

The research is part of the program of the National Laboratory FAMO in Toruń, Poland, and is supported by the Polish National Science Centre Project nos. DEC-2011/01/B/ST2/00491, DEC-2012/05/D/ST2/01914 and DEC-2013/11/D/ST2/02663 as well as by the Foundation for Polish Science TEAM and START Projects which are co-financed by the EU European Regional Development Fund. The research was also supported by the European Regional Development Fund within the Regional Operational Programme for Kujawsko-Pomorskie Voivodeship for the years 2007-2013 and the national budget of Poland (project RPKP 05.04.00-04-006/13). J.T. Hodges was supported by the Greenhouse Gas and Climate Sciences Measurements Program of the National Institute of Standards and Technology.

#237196 - $15.00 USD Received 31 Mar 2015; revised 6 May 2015; accepted 11 May 2015; published 22 May 2015